IEEE Access
Multidisciplinary | Rapid Review | Open Access Journal

Received March 17, 2018, accepted April 15, 2018, date of publication April 23, 2018, date of current version May 16, 2018.

Digital Object Identifier 10.1109/ACCESS.2018.2829207

Bifurcation and Periodic Solutions in Memristive Hyperchaotic System

XIAOYUN ZHONG[1], (Student member, IEEE), MINFANG PENG[1], (Member, IEEE), MOHAMMAD SHAHIDEHPOUR[2], (Fellow, IEEE), AND SHANGJIANG GUO[3]

[1]College of Electrical and Information Engineering, Hunan University, Changsha 410082, China
[2]Electrical and Computer Engineering Department, Illinois Institute of Technology, Chicago, IL 60616, USA
[3]College of Mathematics and Econometrics, Hunan University, Changsha 410082, China

Corresponding author: Minfang Peng (minfangpeng@hnu.edu.cn)

This work was supported in part by the National Nature Science Foundation of China under Grant 61472128 and Grant 11671123 and in part by the Hunan Provincial Natural Science Foundation under Grant 14JJ1025 and Grant 14JJ2150.

ABSTRACT This paper is devoted to a memristive hyperchaotic system. Different from some the existing literature, we derive analytically, under appropriate conditions, the stability and the analytic expression of the Hopf bifurcation by employing center manifold theorem. The system shows dynamics including equilibrium set with one or three elements, Lyapunov exponents with different signs, such as $(0, 0, 0, -)$, $(+, 0, -, -)$, $(+, 0, 0, -)$, and $(+, +, 0, -)$, by varying only one parameter. Moreover, the coexistence of multiple hyperchaotic attractors is observed. Some simulation examples are presented to illustrate our theoretical results.

INDEX TERMS Memristor, hyperchaotic circuit, Lyapunov exponents, periodic solutions, center manifold.

I. INTRODUCTION

Originally, along with the resistor, capacitor and inductor, the memristor is the fourth fundamental circuit element, which has been theoretically postulated [10] and classified [12]. Since 2008, when the researchers at Hewlett-Packard (HP) Labs developed the device [37], the memristor has attracted indispensable attentions from both industry and academia, due to its potential applications in neural networks, novel storage medium, artificial intelligence, chaotic circuit and so on [6], [7], [14], [33].

Recently, the modeling, analysis and design of memristor-based circuit have been studied by many researchers. Owing to the nonlinearity of the memristor element, the memristor-based circuits are able to generate a chaotic signal with ease and reproduce the complicated and unpredictable behavior [1], [4], [6]. In particular, the bifurcation of a mathematical model with only two circuit elements (namely, a memristor and a battery) was studied analytically and numerically [34]. In addition, the bifurcation phenomena in systems were investigated by applying bifurcation theory [9], [19], [41]. Furthermore, memristor-based chaotic circuits and related topics were presented by various authors [13]–[16], [21], [23], [31]–[44]. Different aspects and properties of bifurcating periodic solutions have been studied by various authors. For example, the phenomenon of extreme multi-stability with hidden oscillation was revealed and the coexistence of infinitely many hidden attractors was observed in [5], the criteria for the existence and number of branches of bifurcating periodic solutions was derived in [8] and [25]. Furthermore, the properties of Hopf bifurcation (including the bifurcation direction and stability of bifurcating periodic solutions) were investigated in [22] and [30] by applying the normal form method and center manifold theorem; the analytical study of the periodic solutions of high dimensional systems with dimension over 4 were given in [3] and [26]–[29].

However, the dynamics of multiple chaotic circuits involving memristor have not been thoroughly investigated until now, and some dynamics such as Hopf bifurcation and periodic solutions are still not well understood. In particular, analytic expression of the Hopf bifurcation (Theorem 6(d) in this work) has not been discovered in any memristive system and this fact motivates our work for the paper.

The state-dependent input-output algebraic relationship of first-order active generalized memristor [40] shown in the dashed box of Fig. 1 can be expressed in the following way:

$$\frac{dv_0}{dt} = f(v_0, v_M), \quad i_M = g(v_0, v_M)v_M. \tag{1}$$

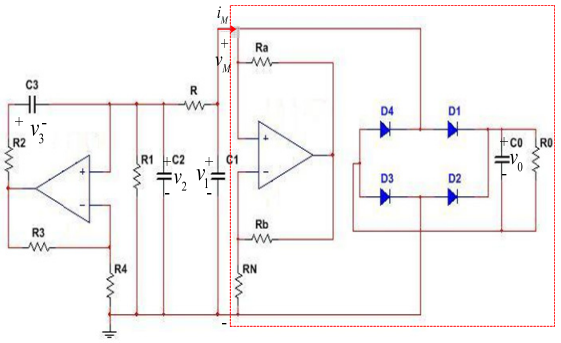

FIGURE 1. The inductor-less hyperchaotic memristor-based circuit.

TABLE 1. Circuit component parameters.

Component	Value
C_0	100 nF
C_1	1 nF
C_2 , C_3	47nF
R_0	1 k Ω
R_1 , R_2	0.2 k Ω
R_3	6.5 k Ω
R_4	3k Ω

The state evolution function $f(\cdot,\cdot)$ and the memductance $g(\cdot,\cdot)$ are given respectively by

$$f(v_0, v_M) = \frac{2I_s[e^{-\rho v_0}\cosh(\rho v_M) - 1]}{C_0} - \frac{v_0}{R_0 C_0},$$
$$g(v_0, v_M) = \frac{2I_s e^{-\rho v_0}\sinh(\rho v_M)}{v_M} - \frac{1}{R_N},$$

where v_M, i_M and v_0 denote the input voltage, the input current and the voltage of C_0, respectively. R_0, C_0 and R_N are parameters of the system and $R_a = R_b$, $\rho = 1/(2nV_T)$, where I_s, n, and V_T denote the reverse saturation current, emission coefficient, and thermal voltage of diode, respectively. $I_s = 6.8913$nA, $n = 1.8268$, and $V_T = 25$ mV.

Based on the memristor, the 4-D state equations of the inductorless hyperchaotic circuit shown in Fig. 1 are derived as

$$\begin{cases} \dfrac{dv_1}{dt} = \dfrac{1}{C_1}[G(v_2 - v_1) - g(v_0, v_1)v_1], \\ \dfrac{dv_2}{dt} = \dfrac{1}{C_2}[Gv_1 - (G + G_1 - kG_2)v_2 - G_2 v_3], \\ \dfrac{dv_3}{dt} = \dfrac{1}{C_3}[G_2(kv_2 - v_3)], \\ \dfrac{dv_0}{dt} = f(v_0, v_1), \end{cases} \tag{2}$$

where v_1, v_2, v_3 and v_0 are the voltages of C_1, C_2, C_3 and C_0, respectively, and $k = R_3/R_4$. The circuit component parameters are summarized in Table 1. Here, the parameters R and R_N are taken as the continuous varied parameters.

In the case of $R_N = 2.5$kΩ and R varying, the authors of [40] investigated the chaotic behavior of (2), the dissipativity, equilibrium points, and stabilities with typical circuit parameters numerically. Surprisingly, the fact that the system (2) may have only one equilibrium point (Theorem 1 in this work) has not been discovered. In this case, we observe multiple chaotic attractors theoretically and numerically and try to seek an analytical form of Hopf bifurcation and periodic solutions of (2).

The rest of this paper is organized as follows. In Section 2, the dynamical behavior of the hyperchaotic memristor circuit described by (2), including its equilibrium numbers, Lyapunov exponents with different signs such as (0, 0, 0, −), (+, 0, −, −), (+, 0, 0, −), (+, +, 0, −) by varying only one parameter, and the bifurcation diagrams with two parameters are derived. It is shown that the system (2) has multiple chaotic attractors spanning from limit cycles of different periodicity to chaotic attractors with various circuit parameters. In Section 3, under appropriate conditions, that zero-Hopf bifurcation (or saddle-node Hopf bifurcation) and analytic expression of the Hopf bifurcation are obtained. Finally, Section 4 presents the conclusion of this study.

II. PRELIMINARY ANALYSIS

To characterize the role of the parameters R, R_N in (2), in this section, we investigate the various dynamical behavior of the system via computer simulations. We analyze the evolution of chaotic attractors through the bifurcation diagrams and Lyapunov exponents. For the sake of illustration, we simplify the presentation by choosing $2 \le R_N \le 5$ and $R > R_N - R_1$.

A. DISSIPATIVITY OF THE SYSTEM

For analysis the dissipativity of (2), we first note that

$$\nabla V = \sum_{j=0}^{3} \frac{\partial \dot{v}_j}{\partial v_j} = -G(v_0, v_1).$$

Here, V is the volume element of the flow and

$$G(v_0, v_1) = 2\rho I_s e^{-\rho v_0}\cosh(\rho v_1)\left(\frac{1}{C_1} + \frac{1}{C_0}\right) + \Lambda,$$

where $\Lambda = \left(\frac{1}{R} - \frac{1}{R_N}\right)\frac{1}{C_1} + \left(\frac{1}{R} + \frac{1}{R_1} - \frac{k}{R_2}\right)\frac{1}{C_2} + \frac{1}{R_0 C_0} + \frac{1}{R_2 C_3}$. If $G(v_0, v_1) > 0$, that is either $\Lambda > 0$ or $\Lambda < 0$ and $v_0 < d(v_1)$, where

$$d(v_1) = \frac{1}{\rho}\log\left[2\rho I_s\cosh(\rho v_1)\left(\frac{1}{C_0} + \frac{1}{C_1}\right)\right] - \frac{1}{\rho}\log(-\Lambda). \tag{3}$$

Then (2) is dissipative with an exponential contraction rate given by $\dot{V} = -G(v_0, v_1)V$. In other words, a volume element V_0 is contracted by the flow into a volume element $V_0 e^{-G(v_0,v_1)t}$ in time t. Thus the system can support attractors.

B. EQUILIBRIUM AND ITS STABILITY

Besides the zero equilibrium, there may be up to two nonzero equilibria, which can be found by solving the following

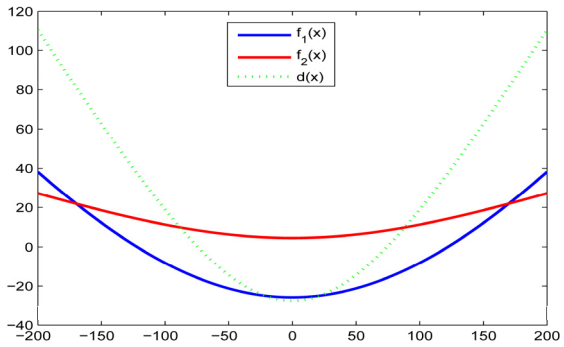

FIGURE 2. Three function curves in the $(x = v_1, v_0)$ plane.

system of nonlinear algebraic equations:

$$\begin{cases} -\dfrac{1}{R}(v_1 - v_2) - \left[2I_s e^{-\rho v_0}\sinh(\rho v_1) - \dfrac{v_1}{R_N}\right] = 0, \\ \dfrac{v_1}{R} - \left(\dfrac{1}{R} + \dfrac{1}{R_1} - \dfrac{k}{R_2}\right)v_2 - \dfrac{v_3}{R_2} = 0, \\ (kv_2 - v_3)\dfrac{1}{R_2} = 0, \\ 2I_s\left[e^{-\rho v_0}\cosh(\rho v_1) - 1\right] - \dfrac{v_0}{R_0} = 0. \end{cases} \tag{4}$$

The algebraic system (4) is not expressed explicitly in terms of any particular parameter due to its nonlinearity. By introducing a new variable $q = \frac{1}{R_N} - \frac{1}{R+R_1}$, and analyzing of (4), we establish that, depending on the values of q, the system (2) may have either only one (if $R = 2.8$) or three (if $R = 4.8$) equilibrium points, as observed in Fig. 2 and confirmed mathematically in Theorem 1.

Theorem 1: Let $R_N \geq 2$, $q = \frac{1}{R_N} - \frac{1}{R+R_1} > 0$ and consider a function on q as

$$S(q) = \frac{1}{\rho}\left(\log\left(\frac{2I_s\rho}{q}\right) - q\right) + 2I_s.$$

(a) *If $S(q) \geq 0$, then the system* (2) *has only an equilibrium* $E_0 = (0, 0, 0, 0)$.

(b) *If $S(q) < 0$, then the system* (2) *has three equilibria E_0, and $E_\pm = (\pm v_1^*, \pm v_2^*, \pm v_3^*, v_0^*)$, where $v_1^* > 0$, $v_2^* > 0$, $v_3^* > 0$, $v_0^* > 0$ satisfy* (4).

Proof: From (4), it follows that the coordinate v_1^* of the equilibria of (2) is a point of intersection of two curves $f_1(x)$ and $f_2(x)$, where

$$f_1(x) = -\frac{1}{\rho}\log\left(\frac{qx}{2I_s\sinh(\rho x)}\right), \quad f_2(x) = \frac{qx}{\tanh(\rho x)} - 2I_s.$$

It is easy to find that both $f_1(x)$ and $f_2(x)$ are even functions, and therefore, we can merely set $x > 0$.

Let $f(x) = f_1(x) - f_2(x)$, $x > 0$. The derivative of $f(x)$ via x implies

$$f'(x) = \frac{\psi(\theta)}{q\theta(\sinh(\theta))^2},$$

where $\theta = \rho x$ and

$$\psi(\theta) = -(\sinh(\theta))^2 + (1-q)\theta\sinh(\theta)\cosh(\theta) + q\theta^2.$$

Suppose that $\vartheta = 2\theta$. It is evident that

$$\psi'(\theta) = q\vartheta + 0.5(1-q)\vartheta\cosh(\vartheta) - 0.5(1+q)\vartheta\sinh(\vartheta) = g(\vartheta)$$

and hence

$$\begin{aligned} g'(\vartheta) &= q - q\cosh(\vartheta) + 0.5(1-q)\vartheta\sinh(\vartheta), \\ g''(\vartheta) &= 0.5(1-3q)\sinh(\vartheta) + 0.5(1-q)\vartheta\cosh(\vartheta), \\ g'''(\vartheta) &= (1-2q)\cosh(\vartheta) + 0.5(1-q)\vartheta\sinh(\vartheta). \end{aligned}$$

As $q = 1/R_N - 1/(R+R_1)$ and the parameter $R_N \geq 2$, we get $q < 0.5$. It follows that $g'''(\vartheta)$ is a monotonically increasing function of ϑ. This leads to $g'''(\vartheta) > g'''(0) = 0$ and hence $g''(\vartheta) > g''(0) = 0, g'(\vartheta) > \psi'(0) = 0, g(\vartheta) > g(0) = 0$, successively. Clearly $f(x)$ is a monotonically increasing function of x. Then we have $\liminf_{x\in(0,+\infty)} f(x) = \lim_{x\to 0^+} f(x) = S(q)$. On the other hand, $\lim_{x\to+\infty} f(x) = +\infty$ and the conclusion follows.

Let $R_N = 2.5$. By Theorem 1, the system (2) with $R = 4.8$ have three equilibrium points $E_0 = (0, 0, 0, 0)$, $E_\pm = (\pm 169.7759, \pm 6.7910, \pm 14.7139, 21.8642)$ since $q = 0.2$ and $S(q) = -30.2199 < 0$. While if $R = 2.8$, then $q = 1/15$ and $S(q) = 82.3060 > 0$, the system (2) has only zero equilibrium E_0 which is unstable.

In general, from a simple analysis by Matlab, we obtain that (2) with $R_N = 2.5$ has only zero equilibrium point if and only if $S(q) > 0$, which is equivalent to $0 < q < q_0$ where $q_0 \approx 0.1509$. Thus the system (2) only has zero equilibrium if and only if parameter $R \in (2.3, 3.8151)$.

It is evident that the system is invariant through mapping: $(v_1, v_2, v_3, v_0) \to (-v_1, -v_2, -v_3, v_0)$, and the system (2) has therefore rotation symmetry about the v_0-axis. It follows that any non-trivial phase portrait of (2) must have a twin phase portrait.

For simplicity, we only consider the zero equilibrium in this paper. For nonzero equilibria, if they exist, the method adopted in this paper can also be applied by using the change of variables such that the equilibrium point can be translated to the origin. For the dynamics around nonzero equilibria, especially the higher codimension bifurcation problems, which cannot be explored analytically, one can use some suitable numerical bifurcation analysis tools, such as MatCont. In the future work, we will use it to calculate the codimension two bifurcation problem.

To study the steady-state bifurcation of the zero equilibrium, one need consider the linearization of (2) at the zero equilibrium. By linearizing (2) at the zero equilibrium, we obtain the following Jacobian matrix

$$\mathbf{A} = \begin{pmatrix} a_1 & a_2 & 0 & 0 \\ b_1 & b_2 & b_3 & 0 \\ 0 & c_2 & c_3 & 0 \\ 0 & 0 & 0 & -d \end{pmatrix},$$

where

$$\begin{cases} a_1 = \left(\frac{1}{R_N} - \frac{1}{R} - 2\rho I_s\right)\frac{1}{C_1}, \quad a_2 = \frac{1}{RC_1}, \\ b_1 = \frac{1}{RC_2}, \ b_2 = -\left(\frac{1}{R} + \frac{1}{R_1} - \frac{k}{R_2}\right)\frac{1}{C_2}, \ b_3 = -\frac{1}{R_2C_2}, \\ c_2 = \frac{k}{R_2C_3}, \quad c_3 = -\frac{1}{R_2C_3}, \quad d = \left(\frac{1}{R_0} + 2\rho I_s\right)\frac{1}{C_0}. \end{cases} \tag{5}$$

Then, the corresponding characteristic equation is given by

$$g(\lambda) = (\lambda + d)(\lambda^3 + p_2\lambda^2 + p_1\lambda + p_0), \tag{6}$$

where

$$\begin{cases} p_2 = -(a_1 + b_2 + c_3), \\ p_1 = a_1b_2 + a_1c_3 + b_2c_3 - b_3c_2 - a_2b_1, \\ p_0 = a_1b_3c_2 + a_2b_1c_3 - a_1b_2c_3. \end{cases} \tag{7}$$

It is easy to show that

$$\begin{cases} a_1 = -\frac{1}{R} + \frac{1}{R_N} - \frac{68913}{456700}, \quad a_2 = \frac{1}{R}, \\ b_1 = \frac{1}{47R}, \quad b_2 = -\frac{1}{47R} + \frac{35}{282}, \ b_3 = -\frac{5}{47}, \\ c_2 = \frac{65}{282}, \quad c_3 = -\frac{5}{47}, \quad d = \frac{23}{200}. \end{cases} \tag{8}$$

By solving the equation $g(\lambda) = 0$, we obtain $\lambda = -d$ is an eigenvalue of matrix $\mathbf{A}$. According to the Routh-Hurwitz condition, not all the roots of $\mathbf{A}$ have negative real parts. For example, for fixed $R_N = 2.5$, when $R = 2.8$, the four eigenvalues of matrix $\mathbf{A}$ are -0.1082, 0.0051 ± 0.0970i, -0.0115, the corresponding equilibrium is unstable. When $R = 3.6365$, the four eigenvalues are -0.0137, -0.0002 ± 0.1000i, -0.0115. In this case, the equilibrium is locally asymptotically stable.

We now explore the stability of the zero equilibrium in general. By some algebra calculations, we have

$$\begin{cases} p_2 = \frac{47}{48R} - \frac{1}{R_N} + m - \frac{5}{282}, \\ p_1 = -\frac{1}{47R_NR} + \frac{5}{282R_N} + \frac{282m - 205}{13254R} \\ \qquad - \left(\frac{5m}{282} - \frac{25}{2209}\right), \\ p_0 = \frac{5}{2209}\left(-\frac{1}{R_NR} - \frac{5}{R_N} + \frac{5+m}{R} + 5m\right), \\ p_2p_1 - p_0 = -\frac{1}{47}\left(\frac{a(R_N)}{R^2} + \frac{b(R_N)}{R} + c(R_N)\right), \end{cases} \tag{9}$$

where $m = 68913/456700 \approx 0.1509$ and $a(R_N)$, $b(R_N)$, $c(R_N)$ are given by

$$\begin{cases} a(R_N) = \frac{48}{47}\left(-\frac{1}{R_N} + m - \frac{205}{282}\right), \\ b(R_N) = \frac{1}{R_N^2} + \frac{1}{R_N}\left(\frac{80}{47} - 2m\right) + m^2 - \frac{80m}{47} + \frac{1925}{79524}, \\ c(R_N) = -\frac{5}{6R_N^2} + \frac{1}{R_N}\left(\frac{5m}{3} - \frac{25}{1692}\right) \\ \qquad - \frac{5}{6}\left(m^2 - \frac{5m}{282} + \frac{25}{2209}\right). \end{cases} \tag{10}$$

Theorem 2: Let E_0 be the zero equilibrium of (2) and $W^s(E_0)$ and $W^u(E_0)$ denote the stable and unstable manifolds of E_0, respectively. Assume that the system parameters satisfies the condition (H): $p_2 > 0, p_0 > 0, p_2p_1 - p_0 > 0$, *then the following assertions hold:*

(a) *If* (H) *is satisfied, then E_0 is locally asymptotically stable with* $\dim W^s(E_0) = 4$.

(b) *If* (H) *is not satisfied, then E_0 is unstable. In particularly, if $p_2 > 0$, $p_0 > 0$, then* $\dim W^s(E_0) = 2$ *and* $\dim W^u(E_0) = 2$.

Proof: Let $\lambda_0 = -d$, λ_1, λ_2, λ_3 be eigenvalues of matrix $\mathbf{A}$ with $\mathrm{Re}(\lambda_1) \le \mathrm{Re}(\lambda_2) \le \mathrm{Re}(\lambda_3)$.

If the condition (H) is satisfied, then the Routh-Hurwitz conditions imply that $\lambda_i < 0$, $i = 0, 1, 2, 3$. By the Hartman-Grobman Theorem we have $\dim W^s(E_0) = 4$ corresponding to the fact that E_0 is stable.

If the condition (H) is not satisfied, then E_0 is unstable. In particular, if $p_2 > 0, p_0 > 0$, then by taking into account the relations between the roots and the polynomial coefficients, we have $\lambda_1 + \lambda_2 + \lambda_3 = -p_2 < 0$, $\lambda_1\lambda_2\lambda_3 = -p_0 < 0$, and $\lambda_1 < 0 \le \mathrm{Re}(\lambda_2) \le \mathrm{Re}(\lambda_3)$. In this case the Routh-Hurwitz conditions indicate that $\lambda_1 < 0$, $\mathrm{Re}(\lambda_2) > 0$, $\mathrm{Re}(\lambda_3) > 0$. From the Hartman-Grobman Theorem we obtain that $\dim W^s(E_0) = 2$ and $\dim W^u(E_0) = 2$. This completes the proof.

From Theorem 2 we know that the stability of the zero equilibrium E_0 may switch, depending on the parameters R and R_N values. An analysis of the roots of $p_0 - p_1p_2$ shows that, for fixed R and R_N, the parameter region

$$\sum = \{(R_N, R) \,|p_0 > 0, p_2 > 0, R_N \ge 2, R \ge 2\}$$

is divided into two parts shown in Fig. 3(a) by the lines R_- and R_+, which are expressed via R_N as

$$R_\pm = \frac{38.2035 + 53.4979R_N - 8.0176R_N^2 \pm 2\sqrt{\Delta}}{63.6725 - 18.0866R_N + 2R_N^2}, \tag{11}$$

where

$$\Delta = 364.8769 - 220.23R_N + 199.6536R_N^2 \\ -50.2241R_N^3 - 6.4053R_N^4,$$

and R_- and R_+ are strictly monotonically increasing functions.

TABLE 2. Distinct Lyapunov exponents of the proposed system with different signs for values of parameter R.

R	LE_1	LE_2	LE_3	LE_4	sign	Dynamical property
3.8	-0.0009	0.0000	-0.0010	-0.0115	(0,0,0,-)	3-torus(quasiperiodic obits)
3.85	0.0030	0.0008	-0.0023	0.0115	(+,0,-,-)	chaos
4	0.0126	-0.0004	-0.0008	-0.0115	(+,0,0,-)	chaos 2-torus
17.5	0.0247	0.0079	-0.0000	-0.6489	(+,+,0,-)	hyperchaos

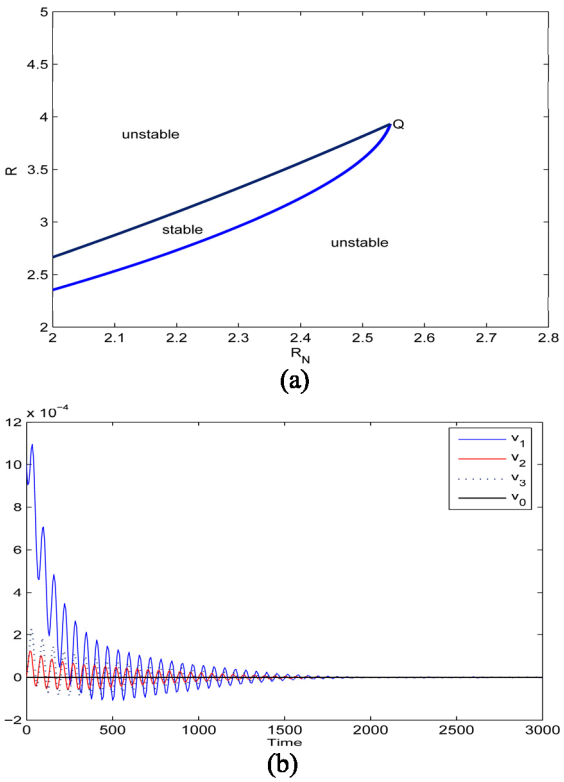

FIGURE 3. (a) Region of stability of E_0 in the $R_N - R$ parameter space. (b) Time series of v_1, v_2, v_3, v_0.

They connect at the point Q with the coordinates (2.5447, 3.9309). By taking into account the mutual positions of the lines R_- and R_+, we find that the equilibrium of (2) is stable for the values of the parameters on the plane (R_N, R) below the line $R+$ and above the line R_-, and unstable for the values of the parameters on the plane (R_N, R) either above the line R_+ or below the line R_-.

The change of stability suggests that a Hopf bifurcation may occur and concrete results shall be explored in Section 3. For each fixed value of the parameter R_N, say $R_N = 2.5$ time series of (2) for the parameter $R = 3.7$ with the initial condition $(0.001, 0, 0, 0)$ converges to $E_0(0, 0, 0, 0)$, as shown in Fig. 3(b) corresponding to the formation of the four roots of the equilibrium $E_0 : -0.0085, -0.0003 \pm 0.1005i, -0.0115$.

C. BIFURCATION ANALYSIS OF THE SYSTEM

Choose $R_N = 2.5$ and take R as a varying parameter within the regions of $2.3 \leq R \leq 50$. For the proposed system, the spectrums of Lyapunov exponents with respect to parameter R are shown in Fig. 4(a). The bifurcation diagram with respect to the varying parameter R for the initial conditions $(\pm 0.01, \pm 0.1, \pm 0.1, 0)$ and computational time 2000s are depicted in Fig. 4(b). It is seen that when R varies on the interval [3.8, 3.845], the first three Lyapunov exponents are all close to zero. This implies the existence of a 3-torus quasiperiodic orbit. When R varies between 3.9 and 4.25, Lyapunov exponent of the proposed system is of sign (+, 0, 0, −) and exhibits 2-torus, while for $R > 8.9$, the first two Lyapunov exponents become positive, which imply that the system is hyperchaotic, as displayed in Fig. 5(d), (e) and (f). These conclusions are also supported by the results shown in Table 2.

In analyzing the dynamical bifurcation and the folding properties of a chaotic attractor, a Poincare map is very significant. Fig. 4(c) and (d) demonstrate projections of the Poincare map of the proposed system in the $v_1 - v_0$ plane for the parameter R varying. It is strongly expected that the system (2) can generate multi-chaos when R varies. This conclusion is also supported by the following results revealed in Fig. 5.

D. COEXISTENCE OF MULTIPLE ATTRACTORS

Coexistence of multiple attractors is an interesting topic [2], [5], [36], [41]. In this subsection, from numerical simulation we study coexistence of multiple attractors of (2). Firstly, perform simulation to observe the interesting phenomenon of multiple chaotic attractors of (2). For the fixed parameters $R = 3.45$ and $R_N = 2.25$, the system (2) can generate two coexisting chaotic attractors, whose phase portraits and time series are shown in Fig. 5. Fig. 5(b) depicts two coexisting chaotic attractors in (v_1, v_0)-plane. The right attractor is a one-periodic chaotic attractor corresponding to initial value (0.0015, 0.001, 0, 0) (blue), and the left is one-periodic chaotic attractor corresponding to initial conditions $(-0.0015, -0.001, 0, 0)$ (red), respectively. We emphasize that the left attractor and the right attractor are diverging completely. For some other choices of parameters, the system (2) also exhibits different multiple strange attractors, such as coexisting multiple hyperchaotic attractors, as shown in Fig. 5(d), and periodic attractors with multiple periodicity.

III. HOPF BIFURCATION AND PERIODIC SOLUTIONS OF THE SYSTEM

In this section, with the help of the higher-dimensional Hopf bifurcation theory and base on symbolic computations,

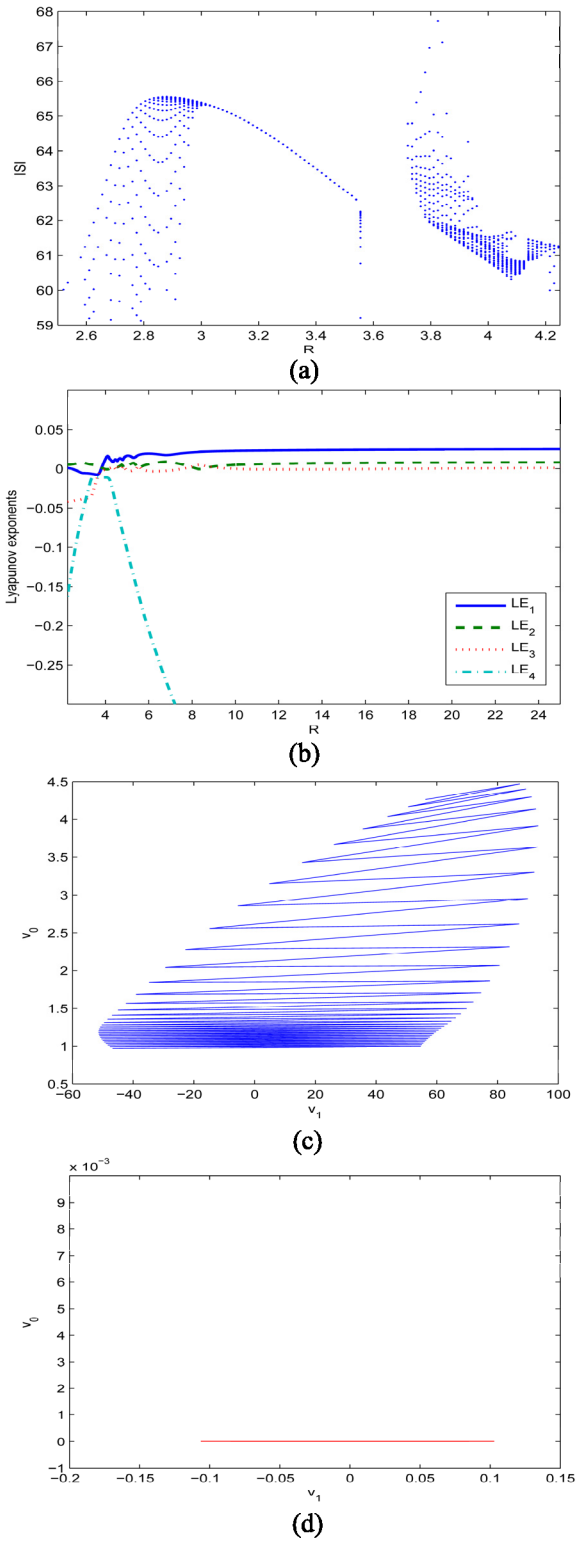

FIGURE 4. (a) Bifurcation diagram. (b) Spectrum of Lyapunov exponents. (c) Poincare map of $v_1 - v_0$ plane with $R = 3.8$. (d) Poincare map of $v_1 - v_0$ plane with $R = 4$, where $R_N = 2.5$ and the initial value $(-0.001, 0, -0.1, 0)$.

dynamical bifurcation with respect to the varying parameters R and R_N shall be investigated. According to the center manifold theory, that zero-Hopf bifurcation occurs when the equilibrium in autonomous system has a zero eigenvalue and a pair of purely imaginary eigenvalues.

Firstly, the existence of Hopf bifurcation is guaranteed by the analysis of characteristic value. For simplicity, we introduce two new variables:

$$\tilde{p}_0 = \frac{(5+m)R_N - 1}{5(1-mR_N)}, \quad \tilde{p}_1 = \frac{(205/282 - m)R_N + 1}{(30/47 - m)R_N + 1}. \tag{12}$$

It is easy to see that $\tilde{p}_1$ is strictly monotonically increasing on the parameter R_N, and $\tilde{p}_1$ has a maximum $\tilde{p}_{1\max} = 1.819$. We note that, under the conditions $5 > R_N \geq 2$, $R \geq R_N - R_1 \geq 1.8$, $p_1 > 0$ is equivalent to $R > 1.2\tilde{p}_1$. Therefore, we can carry out the model analysis with $p_1 > 0$.

Theorem 3: Let $5 > R_N \geq 2$ and $R \geq 1.8$. *Then the following assertions hold.*

(a) *If* $p_0 = 0$ *(that is,* $R = \tilde{p}_0$*, as shown in* (12)*),* $p_2 > 0$*, and* $p_2^2 - 4p_1 < 0$*, then the characteristic equation of* E_0 *has a zero root and three roots with negative real parts, which implies that the system* (2) *may undergo a fixed point bifurcation.*

(b) *If* $p_0 = p_2 = 0$*, then the characteristic equation of* E_0 *has a zero eigenvalue, a negative eigenvalue, and a pair of purely imaginary eigenvalues. In this case, zero-Hopf bifurcation occurs.*

(c) *If* $p_0 p_2 > 0$ *and* $(b(R_N))^2 - 4a(R_N)c(R_N) > 0$*, then as* R *varies and passes through the critical value* $R^* = R_+$ *or* R_-*, a Hopf bifurcation occurs (the stability of* (2) *switches for around* R_- *or* R_+*, where expressions of* p_0*,* p_1*,* p_2*,* $a(R_N)$*,* $b(R_N)$*,* $c(R_N)$*, and* $R_\pm$ *are given in* (9)-(11).

Proof: Suppose that the zero equilibrium in (2) has a pure imaginary root $i\omega_0$ in which $\omega_0 > 0$. We obtain

$$p_0 - p_2\omega_0^2 + i\omega_0\left(p_1 - \omega_0^2\right) = 0.$$

Separating the real and imaginary parts, we find that the variable ω_0 is given by the following equations:

$$\omega_0^2 = \frac{p_0}{p_2}, \quad \omega_0^2 = p_1.$$

Thus, $p_0 - p_1 p_2 = 0$. From the representation (9) of $p_0 - p_1 p_2$ via R, R_N, we obtain that the critical value $R = R^*$ equals to either R_+ or R_- as

$$R_\pm = \frac{-b(R_N) \pm \sqrt{b(R_N)^2 - 4a(R_N)c(R_N)}}{2c(R_N)},$$

where $a(R_N)$, $b(R_N)$, $c(R_N)$ are given by (10). It follows that by direct computation and with the help of Matlab tool, we obtain approximate expression of $R_\pm$, as shown in (11).

Substituting $R = R^*$ into the characteristic equation (6), we have $\lambda_1 = i\omega_0$, $\lambda_2 = -i\omega_0$, $\lambda_3 = -p_2$, $\lambda_4 = -d$, where $\omega_0 = \sqrt{p_1}$. Hence, in the case of $p_0 p_2 > 0$, the first condition for Hopf bifurcation [17] is satisfied.

From the characteristic equation (6) and the relations $p_1 = \omega_0^2$ and $\Delta > 0$, it follows that

$$(3\lambda + 2\lambda P_2 + p_1)\frac{\partial \lambda}{\partial R} + \lambda^2 \frac{\partial p_2}{\partial R} + \lambda \frac{\partial p_1}{\partial R} + \frac{\partial p_0}{\partial R} = 0.$$

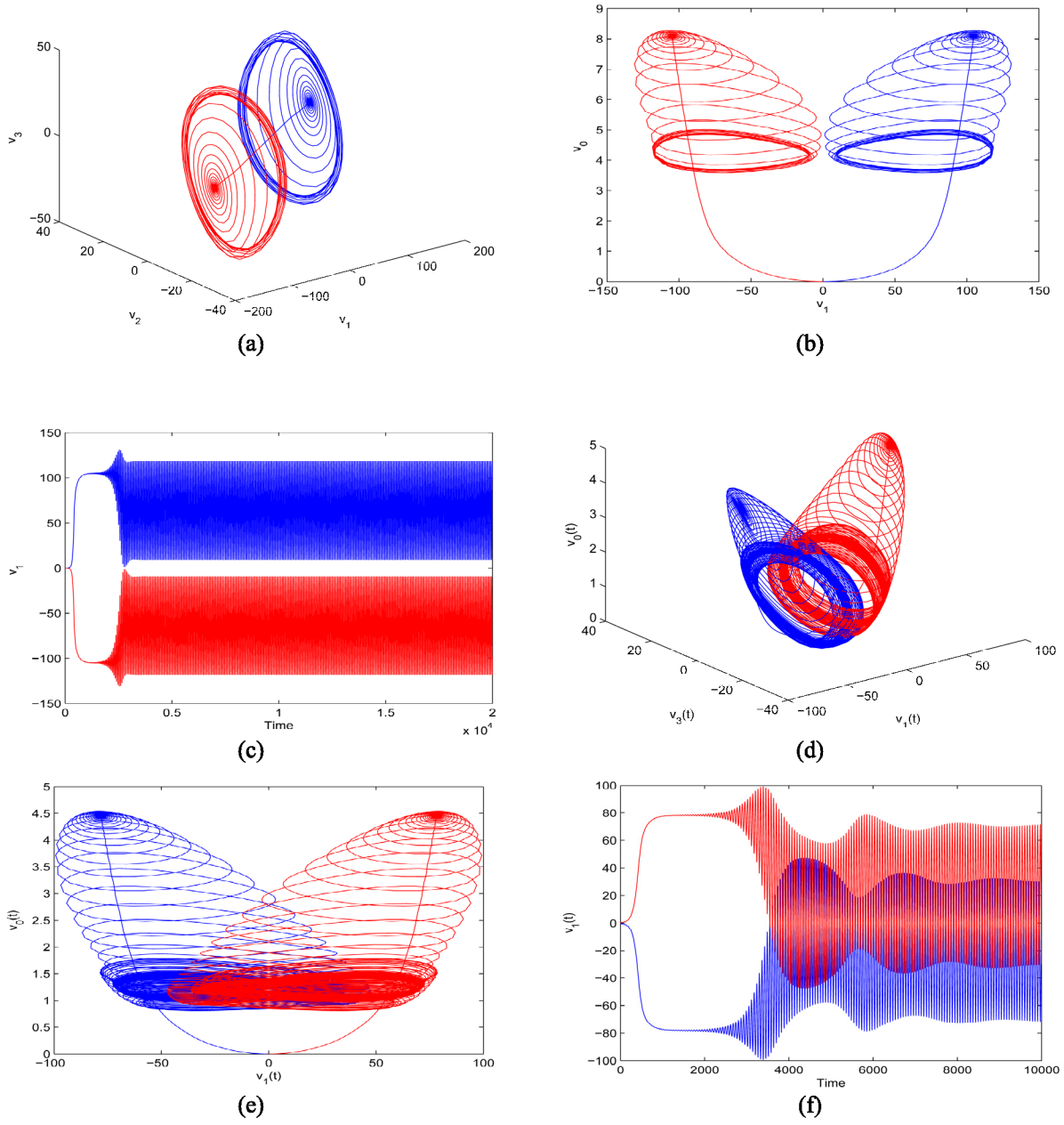

FIGURE 5. Multiple chaotic attractors: (a) $v_1 - v_2 - v_3$ and (b) $v_1 - v_0$ plane; (c) Time series of v_1 for $R = 3.45$, $R_N = 2.25$, the initial conditions (0.0015, 0.001, 0, 0) (blue) and (−0.0015, −0.001, 0, 0) (red). Multiple chaotic attractors: (d) $v_1 - v_3 - v_0$ and (e) $v_1 - v_0$ plane, (f) Time series of v_1 for $R = 4$, $R_N = 2.5$, the initial conditions (0.001, 0, 0.1, 0) (red) and (−0.001, 0, −0.1, 0) (blue).

A simple calculation is given as

$$\begin{aligned}
&\mathrm{Re}\left(\frac{\partial\lambda}{\partial R}\Big|_{R=R^*,\lambda=i\omega_0}\right)\\
&= -\mathrm{Re}\left(\frac{\lambda^2\frac{\partial p_2}{\partial R}+\lambda\frac{\partial p_1}{\partial R}+\frac{\partial p_0}{\partial R}}{3\lambda+2\lambda P_2+p_1}\Big|_{R=R^*,\lambda=i\omega_0}\right)\\
&= -\frac{\left(\frac{\partial p_0}{\partial R}-\omega_0^2\frac{\partial p_2}{\partial R}\right)\left(p_1-3\omega_0^2\right)+2\omega_0^2 p_2\frac{\partial p_1}{\partial R}}{\left(p_1-3\omega_0^2\right)^2+\left(2\omega_0 p_2\right)^2}\Big|_{R=R^*}\\
&= -\frac{\frac{\partial\left(p_1p_2-p_0\right)}{\partial R}}{\left(2p_1+p_2^2\right)}\Big|_{R=R^*} \neq 0. \qquad (13)
\end{aligned}$$

Therefore, the condition for the occurrence of a Hopf bifurcation [17] is also satisfied. This implies that Hopf bifurcation for (2) exists.

Remark 4: From Theorem 3, Hopf bifurcation occurs at a set of parameter values given by

$$H = \{(R, R_N)\,|R = R_\pm \text{ or } R = \tilde{p}_0, 2 \le R_N \le 2.5447\},$$

where $R_\pm$, $\tilde{p}_0$ as shown in (11)-(12).

Remark 5: Recall the codimension is the number of independent conditions characterizing the bifurcation problem. The codimension two zero-Hopf bifurcation is different from codimension one Hopf bifurcation(See, for example, [24]). In fact, if the bifurcation is characterized by one independent conditions, then it is called codimension one bifurcation. While a bifurcation characterized by two independent conditions is called codimension two bifurcation. Theorem 3(b) presents some parameter conditions for such a codimension two bifurcation as zero-Hopf bifurcation. Fig. 6 shows the bifurcation diagram of (2) with $R_N = 2.5$, and the H point indicates that Hopf bifurcation will occur at the corresponding parameter value. The corresponding parameter values of the two H points are $R = 3.5990$ and $R = 4.2727$, respectively. Results are consistent with the conclusion of theorem 3(c).

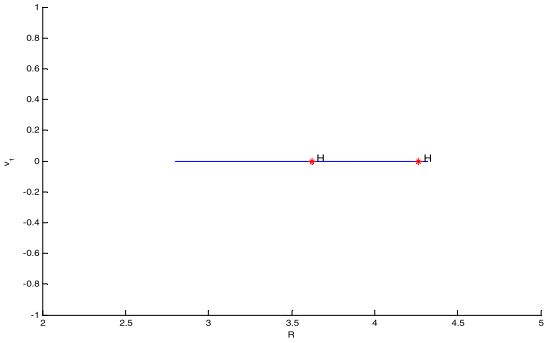

FIGURE 6. The bifurcation diagram of the system (2) with $R_N = 2.5$.

We now turn to investigate the stability and seek Hopf bifurcation and periodic solutions of (2) at E_0 by employing the normal form theory [18], [20], [24] and we obtain analytical formulae for the normal form coefficients from (2) derived via the center manifold reduction that give detailed information about the bifurcation and stability of various bifurcated solutions [19], [38].

Let

$$\xi_1 = \begin{pmatrix} a_2\left(a_1c_3+\omega_0^2\right) - i\omega_0\left(a_1-c_3\right) \\ -c_3\left(a_1^2+\omega_0^2\right) - i\omega_0\left(a_1^2+\omega_0^2\right) \\ c_2\left(a_1^2+\omega_0^2\right) \\ 0 \end{pmatrix},$$

$$\xi_3 = \begin{pmatrix} a_2\left(c_3+p_2\right) \\ -\left(c_3+p_2\right)\left(a_1+p_2\right) \\ c_2\left(a_1+p_2\right) \\ 0 \end{pmatrix}, \quad \text{and } \xi_0 = \begin{pmatrix} 0 \\ 0 \\ 0 \\ 1 \end{pmatrix}.$$

Then

$$\mathbf{A}\xi_1 = i\omega_0\xi_1, \quad \mathbf{A}\xi_3 = -p_2\xi_3, \quad \mathbf{A}\xi_0 = -d\xi_0.$$

In order to study properties of the solutions of (2), by changing the variables

$$(v_1, v_2, v_3, v_0)^T = \mathbf{T}(x, y, z, w)^T,$$

where

$$\mathbf{T} = (\mathrm{Re}\xi_1, -\mathrm{Im}\xi_1, \xi_3, \xi_0). \tag{14}$$

From the Taylor expansions of $e^{-\rho v_0}$, $\sinh(\rho v_1)$ and $\cosh(\rho v_1)$, we can rewrite (2) as

$$\begin{cases} \dot{x} = -\omega_0 y + F_1(x, y, z, w), \\ \dot{y} = \omega_0 x + F_2(x, y, z, w), \\ \dot{z} = -p_2 z + F_3(x, y, z, w), \\ \dot{w} = -dw + F_4(x, y, z, w), \end{cases}$$

where

$$\begin{aligned} &F_i(x, y, z, w) \\ &= \rho^2\gamma_i\left(\left(w - \frac{\rho}{2}w^2\right)\left(p_{11}x + p_{12}y + p_{13}z\right)\right. \\ &\qquad \left. -\frac{\rho}{6}\left(p_{11}x + p_{12}y + p_{13}z\right)^3 + \cdots\right), \quad i = 1, 2, 3, \\ &F_4(x, y, z, w) \\ &= \frac{\rho^2}{2}\left(w^2 - \frac{\rho}{3}w^3 + \left(p_{11}x + p_{12}y + p_{13}z\right)^2\right. \\ &\qquad \left. -\rho w\left(p_{11}x + p_{12}y + p_{13}z\right)^2 + \cdots\right) \end{aligned}$$

in which $p_{11} = a_2(a_1c_3 + \omega_0^2), p_{12} = \omega_0(a_1 - c_3), p_{13} = a_2(c_3 + p_2)$ and

$$\begin{cases} \gamma_1 = 2I_sc_2(a_1^2 + \omega_0^2)(a_1 + p_2)/\mathrm{P}, \\ \gamma_2 = -2I_sc_2(a_1 - c_3)(a_1 + p_2)/\mathrm{P}, \\ \gamma_3 = -2I_s\left[(a_1 - c_3)(c_3 + p_2)(a_1 + p_2)\right. \\ \qquad \left. + a_2(a_1^2 + \omega_0^2)(c_3 + p_2)\right]/\mathrm{P}, \end{cases} \tag{15}$$

where

$$\begin{aligned} \mathrm{P} = &a_2c_2(a_1c_3 + \omega_0^2)(a_1^2 + \omega_0^2)(a_1 + p_2) \\ &- c_2(a_1^2 + \omega_0^2)(a_1 - c_3)(c_3 + p_2)(a_1 + p_2) \\ &- a_2c_2(a_1^2 + \omega_0^2)^2(c_3 + p_2) \\ &+ c_2c_3(a_1 - c_3)(a_1^2 + \omega_0^2)(a_1 + p_2). \end{aligned}$$

Thus one can calculate the following characteristic quantities:

$$\begin{aligned} g_{11} &= g_{02} = g_{20} = 0, \\ G_{21} &= -\frac{\rho^3}{8}\left[\gamma_1(p_{11}^3 + p_{11}p_{12}^2) + \gamma_2(p_{11}^2p_{12} + p_{13}^3)\right] \\ &\quad - \frac{\rho^3}{8}i\left[\gamma_2(p_{11}^3 + p_{11}p_{12}^2) - \gamma_1(p_{11}^2p_{12} + p_{13}^3)\right], \end{aligned}$$

and

$$\begin{aligned} h_{11}^1 &= h_{20}^1 = 0, \quad h_{11}^2 = \frac{\rho^2}{4}(p_{11}^2 + p_{12}^2), \\ h_{20}^2 &= \frac{\rho^2}{4}(p_{11}^2 - p_{12}^2 - 2ip_{11}p_{12}). \end{aligned}$$

Now, we define α_{11}, α_{20} in the following way

$$D\alpha_{11} = -h_{11}, (D - 2i\omega_0)\alpha_{20} = -h_{20},$$

where

$$D = \begin{pmatrix} -p_2 & 0 \\ 0 & -d \end{pmatrix}, \quad h_{11} = \begin{pmatrix} h_{11}^1 \\ h_{11}^2 \end{pmatrix}, \quad h_{20} = \begin{pmatrix} h_{20}^1 \\ h_{20}^2 \end{pmatrix}.$$

As a result, we obtain

$$\alpha_{11} = \begin{pmatrix} 0 \\ \frac{\rho^2}{4p_2}(p_{11}^2 + p_{12}^2) \end{pmatrix},$$
$$\alpha_{20} = \begin{pmatrix} 0 \\ \frac{\rho^2}{4(d+2\omega_0 i)}(p_{11}^2 - p_{12}^2 - 2ip_{11}p_{12}) \end{pmatrix}.$$

In addition, we have $G_{110}^1 = G_{101}^1 = 0$ and

$$G_{110}^2 = \frac{\rho^2}{2}[(\gamma_1 p_{11} + \gamma_2 p_{12}) + i(\gamma_2 p_{11} - \gamma_1 p_{12})],$$
$$G_{101}^2 = \frac{\rho^2}{2}[(\gamma_1 p_{11} - \gamma_2 p_{12}) + i(\gamma_2 p_{11} + \gamma_1 p_{12})].$$

It follows that

$$\begin{aligned} g_{21} &= G_{21} + \sum_{k=1}^{2}(2G_{110}^k\alpha_{11}^k + G_{101}^k\alpha_{20}^k) \\ &= -\frac{\rho^3}{8}\left[\gamma_1(p_{11}^3 + p_{11}p_{12}^2) + \gamma_2(p_{11}^2p_{12} + p_{13}^3)\right] \\ &\quad + \frac{\rho^4}{4}\left[\frac{2\kappa(\gamma_1 p_{11} + \gamma_2 p_{12})}{p_2}\right. \\ &\quad \left. + \frac{(k_1k_2 - l_1l_2)d + 2\omega_0(k_1l_2 + k_2l_1)}{d^2 + 4p_1}\right] \\ &\quad + i\left\{-\frac{\rho^3}{8}\left[\gamma_2(p_{11}^3 + p_{11}p_{12}^2) - \gamma_1(p_{11}^2p_{12} + p_{13}^3)\right]\right. \\ &\quad + \frac{\rho^4}{4}\left[\frac{2\kappa(\gamma_2 p_{11} - \gamma_1 p_{12})}{p_2}\right. \\ &\quad \left.\left. + \frac{(k_1l_2 + k_2l_1)d - 2\omega_0(k_1k_2 - l_1l_2)}{d^2 + 4p_1}\right]\right\} \end{aligned}$$

in which $\kappa = p_{11}^2 + p_{12}^2$, $k_1 = p_{11}^2 - p_{12}^2$, $k_2 = \gamma_1 p_{11} - \gamma_2 p_{12}$, $l_1 = -2p_{11}p_{12}$, $l_2 = \gamma_2 p_{11} + \gamma_1 p_{12}$.

Based on the above analysis, the curvature coefficient of limit cycle in (2) can be given by the following formula

$$C_1(0) = \frac{i}{2\omega_0}\left(g_{20}g_{11} - 2|g_{11}|^2 - \frac{1}{3}|g_{02}|^2\right) + \frac{1}{2}g_{21} = \frac{1}{2}g_{21}.$$

Moreover, we have

$$\mu_2 = -\frac{\mathrm{Re}(C_1(0))}{\alpha'(0)}, \quad \tau_2 = -\frac{\mathrm{Im}(C_1(0)) + \mu_2\omega'(0)}{\omega_0},$$
$$\beta_2 = 2\mathrm{Re}(C_1(0)),$$

where

$$\begin{aligned} \alpha'(0) &= \mathrm{Re}\left(\frac{\partial\lambda}{\partial R}\Big|_{R=R^*,\lambda=i\omega_0}\right) = -\frac{\frac{\partial(p_1p_2 - p_0)}{\partial R}}{2p_1 + p_2^2}\Big|_{R=R^*} \\ &= -\frac{1}{98(p_1 + p_2^2)}\left(\frac{2a(R_N)}{R^3} + \frac{b(R_N)}{R^2}\right)\Big|_{R=R^*}, \\ \omega'(0) &= \mathrm{Im}\left(\frac{\partial\lambda}{\partial R}|_{R=R^*,\lambda=i\omega_0}\right) = \frac{1}{\omega_0}\left[p_2\alpha'(0) + \frac{1}{2}\frac{\partial p_1}{\partial R}\right]\Big|_{R=R^*} \\ &= \frac{1}{\omega_0}\left[p_2\alpha'(0) + \frac{1}{98R^2}\left(\frac{1}{R_N} + \frac{15942489}{21464900}\right)\right]\Big|_{R=R^*}. \end{aligned}$$

Furthermore, we obtain the period and characteristic exponent as

$$T = \frac{2\pi}{\omega_0}(1 + \tau_2\varepsilon^2 + O(\varepsilon^4)), \quad \beta = \beta_2\varepsilon^2 + O(\varepsilon^4),$$

where $\varepsilon^2 = \frac{R - R^*}{\mu_2} + O((R - R^*)^2)$ and the expression of the bifurcating periodic solution of (2) is (except for an arbitrary phase angle)

$$\begin{aligned} x &= \mathrm{Re}u, \quad y = \mathrm{Im}u, \quad (z, w)^T \\ &= \alpha_{11}|u| + \mathrm{Re}\left(\alpha_{20}u^2\right) + O(|u|^3), \end{aligned}$$

and

$$\begin{aligned} u &= \varepsilon e^{\frac{2\pi t}{T}i} + \frac{i\varepsilon^2}{6\omega_0}\left(g_{02}e^{-\frac{4\pi t}{T}i} - 3g_{20}e^{-\frac{4\pi t}{T}i} + 6g_{11}\right) + O(\varepsilon^3) \\ &= \varepsilon e^{\frac{2\pi t}{T}i} + O(\varepsilon^3). \end{aligned}$$

By tedious calculation, we obtain a bifurcating periodic solution of (2) as (16), as shown at the bottom of this page, where a_1, a_2, c_3, d, p_0, p_1, p_2 as shown in (8)-(9) and K is defined as

$$\begin{aligned} K &= \frac{\rho^2}{4(d^2 + 4p_1)}\left[(p_{11}^2 - p_{12}^2)d - 2\omega_0 p_{11}p_{12}\right]\cos\left(\frac{4\pi t}{T}\right) \\ &\quad + 2\left[(p_{11}^2 - p_{12}^2)\omega_0 + p_{11}p_{12}d\right]\sin\left(\frac{4\pi t}{T}\right). \end{aligned}$$

Summing up the results obtained above, the assertions in Theorem 6 below are established.

Theorem 6: Fix R_N and let the parameter R vary such that $R > R_N - R_1$ and $p_0p_2 > 0$. Then the following assertions hold for periodic solutions of (2), which emerge from E_0 via Hopf bifurcation near the critical value R^*.

(a) *If $\mu_2 > 0$, then a branch of bifurcating periodic solutions of (2) exists for sufficient small $|R - R^*|$. In this*

$$\begin{pmatrix} v_1 \\ v_2 \\ v_3 \\ v_4 \end{pmatrix} = \begin{pmatrix} \omega_0(a_1 - c_3)\sin\left(\frac{2\pi t}{T}\right) + a_2\left(a_1c_3 + \omega_0^2\right)\cos\left(\frac{2\pi t}{T}\right) \\ \omega_0\left(a_1^2 + \omega_0^2\right)\sin\left(\frac{2\pi t}{T}\right) - c_3\left(a_1^2 + \omega_0^2\right)\cos\left(\frac{2\pi t}{T}\right) \\ c_2\left(a_1^2 + \omega_0^2\right)\cos\left(\frac{2\pi t}{T}\right) \\ \frac{\rho^2}{4p_2}\left(p_{11}^2 + p_{12}^2\right) \end{pmatrix}\varepsilon + \begin{pmatrix} 0 \\ 0 \\ 0 \\ K \end{pmatrix}\varepsilon^2 + O\left(\varepsilon^3\right), \tag{16}$$

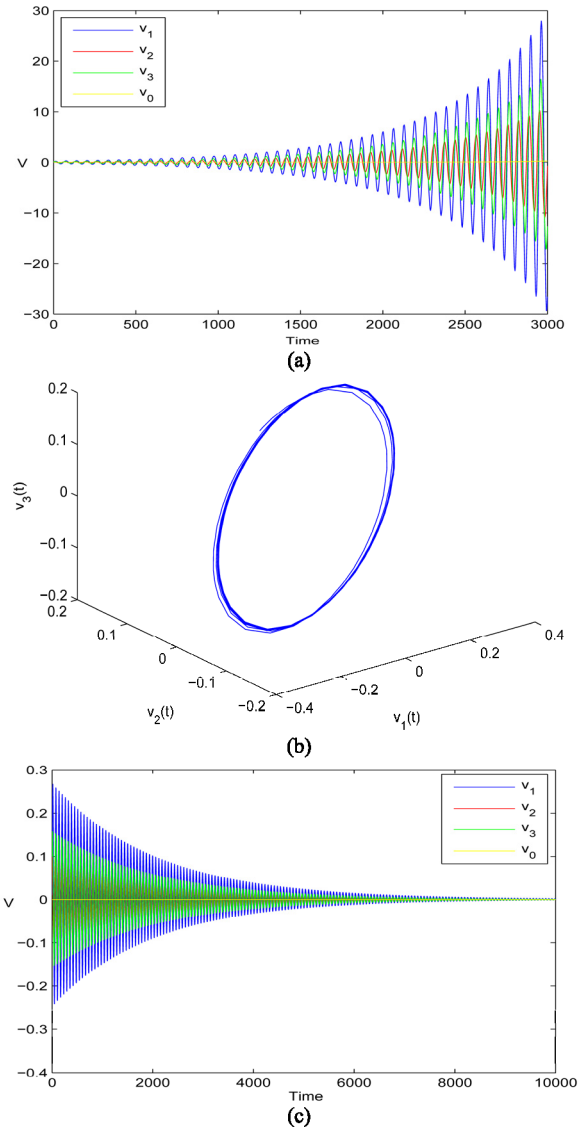

FIGURE 7. Solutions of the system (2) with the parameter $R_N = 2.5$ and the initial value (0.01, 0.1, 0.1, 0). (a) $R = 3.3$. (b) $R = 3.5865$. (c) $R = 3.81$.

case, the Hopf bifurcation is non-degenerate and subcritical, and this branch of periodic solutions is unstable.

(b) *If* $\mu_2 < 0$, *then a branch of bifurcating periodic solutions of* (2) *exists for sufficient small* $|R-R^*|$. *In this case, this branch of periodic solutions of* (2) *from Hopf bifurcation at* E_0 *is non-degenerate, supercritical and stable.*

(c) *The period and a nonzero Floquet exponent of the bifurcating periodic solution of* (2) *are:*

$$T = \frac{2\pi}{\omega_0}(1 + \tau_2\varepsilon^2 + O(\varepsilon^4)), \quad \beta = \beta_2\varepsilon^2 + O(\varepsilon^4),$$

where $\mu_2 = -\frac{\mathrm{Re}(C_1(0))}{\alpha'(0)}$, $\tau_2 = -\frac{\mathrm{Im}(C_1(0))+\mu_2\omega'(0)}{\omega_0}$, $\beta_2 = 2\mathrm{Re}(C_1(0))$, $\varepsilon^2 = \frac{R-R^*}{\mu_2} + O((R-R^*)^2)$.

(d) *The expression of the periodic solution of* (2) *from Hopf bifurcation has the form as* (16).

To illustrate that the analytical results are valid, we consider some examples from the numerical simulation. Fix $R_N = 2.5$ in (2) one can calculate $R_- = 3.5990$, $R_+ = 4.2727$, $\beta_2 = -3.3317e-010$ and $\mu_2 = 1.3348e-012$ when the critical value $R^* = R_-$, which implies that Hopf bifurcation of (2) at E_0 is non-degenerate and supercritical, and a bifurcating periodic solution exists for this case, which is stable, as depicted in Fig. 7(b). When the parameter $R < R_-$ (or $R_- < R < 3.8143$), simulations show that E_0 is unstable (or stable), as shown in Fig. 7(a) (or (c)), respectively. These are in good agreement with results of Theorems 6 and 3.

IV. CONCLUSION

In this paper, we studied a hyperchaotic memristor system. Different from some existing literature, we derive, under appropriate conditions, the stability and analytic expression of the Hopf bifurcation in terms of center manifold theorem. We prove that equilibrium set of the proposed system has one or three elements. This new memristor system has a simple structure but exhibits complex dynamical behavior, including 3-torus (quasiperiodic orbits), 2-torus, chaos and hyperchaos. It also exhibits coexisting multiple hyperchaotic attractors. We calculate and obtain analytical form of bifurcating periodic solutions. It shows the periodic solution can be determined with respect to the system parameters R_N and R. Moreover, in terms of the characteristic equation, we verify that under some appropriate conditions, zero-Hopf bifurcation occurs. These results are new and improve some known results, and can act as a guidance for doing further work. It is an interesting open problem to analyze whether or not the uniqueness of the periodic solution can be proved, which leads to the future studying.

ACKNOWLEDGMENT

The authors would like to thank the editors and anonymous reviewers for their careful work and thoughtful suggestions that have helped improve this paper substantially.

REFERENCES

[1] S. P. Adhikari, M. P. Sah, H. Kim, and L. O. Chua, "Three fingerprints of memristor," *IEEE Trans. Circuits Syst. I, Reg. Papers*, vol. 60, no. 11, pp. 3008–3021, Nov. 2013.

[2] N. H. Alombah, H. Fotsin, and K. Romanic, "Coexistence of multiple attractors, metastable chaos and bursting oscillations in a multiscroll memristive chaotic circuit," *Int. J. Bifurcation Chaos*, vol. 27, no. 5, pp. 1–20, 2017.

[3] P. Amster and R. Balderrama, "Existence and multiplicity of periodic solutions for a generalized hematopoiesis model," *J. Appl. Math. Comput.*, vol. 55, nos. 1–2, pp. 591–607, 2017.

[4] A. Ascoli and F. Corinto, "Memristor models in a chaotic neural circuit," *Int. J. Bifurcation Chaos*, vol. 23, no. 3, pp. 1–28, 2013.

[5] B. C. Bao, H. Bao, N. Wang, M. Chen, and Q. Xu, "Hidden extreme multistability in memristive hyperchaotic system," *Chaos, Solitons Fractals*, vol. 94, pp. 102–111, Jan. 2017.

[6] J. Borghetti, G. S. Snider, P. J. Kuekes, and J. J. Yang, "'Memristive' switches enable 'stateful' logic operations via material implication," *Nature*, vol. 464, pp. 873–876, Apr. 2010.

[7] A. Buscarino, L. Fortuna, M. Frasca, L. V. Gambuzza, and G. Sciuto, "Memristive chaotic circuits based on cellular nonlinear networks," *Int. J. Bifurcation Chaos*, vol. 22, pp. 1–13, Mar. 2012.

[8] J. Cao, R. Yuan, H. Jiang, and J. Song, "Hopf bifurcation and multiple periodic solutions in a damped harmonic oscillator with delayed feedback," *J. Comput. Appl. Math.*, vol. 263, pp. 14–24, Jun. 2014.

[9] Y. Chang, X. Wang, and D. Xu, "Bifurcation analysis of a power system model with three machines and four buses," *Int. J. Bifurcation Chaos*, vol. 26, pp. 1–12, May 2016.
[10] L. Chua, "Memristor-the missing circuit element," *IEEE Trans. Circuit Theory*, vol. CT-18, no. 5, pp. 507–519, Sep. 1971.
[11] L. O. Chua, "The fourth element," *Proc. IEEE*, vol. 100, no. 6, pp. 1920–1927, Jun. 2012.
[12] L. O. Chua and S. M. Kang, "Memristive devices and systems," *Proc. IEEE*, vol. 64, no. 2, pp. 209–223, Feb. 1976.
[13] T. Driscoll, Y. V. Pershin, D. N. Basov, and M. Di Ventra, "Chaotic memristor," *Appl. Phys. A, Solids Surf.*, vol. 102, no. 4, pp. 885–889, 2011.
[14] K. Eshraghian, K.-R. Cho, O. Kavehei, S.-K. Kang, D. Abbott, and S.-M. S. Kang, "Memristor MOS content addressable memory (MCAM): Hybrid architecture for future high performance search engines," *IEEE Trans. Very Large Scale Integr. (VLSI) Syst.*, vol. 19, no. 8, pp. 1407–1417, Aug. 2011.
[15] A. M. A. El-Sayed, H. M. Nour, A. Elsaid, A. E. Matouk, and A. Elsonbaty, "Circuit realization, bifurcations, chaos and hyperchaos in a new 4D system," *Appl. Math. Comput.*, vol. 239, pp. 333–345, Jul. 2014.
[16] A. L. Fitch, D. S. Yu, H. H. C. Iu, and V. Sreeram, "Hyperchaos in a memristor-based modified canonical Chua's circuit," *Int. J. Bifurcation Chaos*, vol. 22, pp. 125–133, Jun. 2012.
[17] J. Guckenheimer and P. Holmes, *Nonlinear Oscillations, Dynamical Systems, and Bifurcation of Vector Field*. New York, NY, USA: Springer-Verlag, 1983.
[18] S. Guo and J. Wu, *Bifurcation Theory of Functional Differential Equations*. New York, NY, USA: Springer-Verlag, 2013.
[19] S. Guo, Y. Chen, and J. Wu, "Two-parameter bifurcations in a network of two neurons with multiple delays," *J. Differ. Equ.*, vol. 244, no. 2, pp. 444–486, 2008.
[20] B. Hassard, N. Kazarinoff, and Y.-H. Wan, *Theory and Application of Hopf Bifurcation*. Cambridge, U.K.: Cambridge Univ. Press, 1982.
[21] M. Itoh and L. O. Chua, "Memristor oscillators," *Int. J. Bifurcation Chaos*, vol. 18, pp. 3138–3206, Nov. 2008.
[22] J. Jia and L. Li, "Hopf bifurcation and periodic solution of a delayed predator-prey-mutualist system," *Adv. Differ. Equ.*, vol. 2016, no. 1, p. 193, 2016.
[23] H. Kim, M. P. Sah, C. Yang, S. Cho, and L. O. Chua, "Memristor emulator for memristor circuit applications," *IEEE Trans. Circuits Syst. I, Reg. Papers*, vol. 59, no. 10, pp. 2422–2431, Oct. 2012.
[24] Y. A. Kuznetsov, *Elements of Applied Bifurcation Theory*. New York, NY, USA: Springer-Verlag, 1998.
[25] G. M. Mahmoud, "Periodic solutions of strongly non-linear Mathieu oscillators," *Int. J. Non-Linear Mech.*, vol. 32, no. 6, pp. 1177–1185, 1997.
[26] G. M. Mahmoud, "Approximate solutions of a class of complex nonlinear dynamical systems," *Phys. A, Stat. Mech. Appl.*, vol. 253, nos. 1–4, pp. 211–222, 1998.
[27] G. M. Mahmoud and S. A. Aly, "Periodic attractors of complex damped non-linear systems," *Int. J. Non-Linear Mech.*, vol. 35, no. 2, pp. 309–323, 2000.
[28] G. M. Mahmoud, M. E. Ahmed, and N. Sabor, "On autonomous and nonautonomous modified hyperchaotic complex Lü systems," *Int. J. Bifurcation Chaos*, vol. 21, pp. 1913–1926, Jul. 2011.
[29] G. M. Mahmoud, E. E. Mahmoud, and A. A. Arafa, "Passive control of n-dimensional chaotic complex nonlinear systems," *J. Vibrat. Control*, vol. 19, no. 7, pp. 1061–1071, 2013.
[30] G. M. Mahmoud, A. A. Arafa, and E. E. Mahmoud, "Bifurcations and chaos of time delay Lorenz system with dimension $2n + 1$," *Eur. Phys. J. Plus*, vol. 132, no. 11, pp. 461–481, Nov. 2017.
[31] B. Muthuswamy and L. O. Chua, "Simplest chaotic circuit," *Int. J. Bifurcation Chaos*, vol. 20, pp. 1567–1580, May 2010.
[32] B. Muthuswamy and P. P. Kokate, "Memristor-based chaotic circuits," *IETE Techn. Rev.*, vol. 26, pp. 417–429, Sep. 2009.
[33] Y. V. Pershin and M. Di Ventra, "Experimental demonstration of associative memory with memristive neural networks," *Neural Netw.*, vol. 23, no. 7, pp. 881–886, 2010.
[34] M. P. D. Sah, Z. I. Mannan, H. Kim, and L. Chua, "Oscillator made of only one memristor and one battery," *Int. J. Bifurcation Chaos*, vol. 25, pp. 1–28, Mar. 2015.
[35] M. da C. Scarabello and M. Messias, "Bifurcations leading to nonlinear oscillations in a 3D piecewise linear memristor oscillator," *Int. J. Bifurcation Chaos*, vol. 24, no. 1, pp. 1–18, 2014.
[36] J. P. Singh and B. K. Roy, "Coexistence of asymmetric hidden chaotic attractors in a new simple 4-D chaotic system with curve of equilibria," *Optik-Int. J. Light Electron Opt.*, vol. 145, pp. 209–217, Sep. 2017.
[37] D. B. Strukov, G. S. Snider, D. R. Stewart, and R. S. Williams, "The missing memristor found," *Nature*, vol. 453, pp. 80–83, May 2008.
[38] Q. Yang and Y. Liu, "A hyperchaotic system from a chaotic system with one saddle and two stable node-foci," *J. Math. Anal. Appl.*, vol. 360, no. 1, pp. 293–306, 2009.
[39] D. Yu, H. H.-C. Iu, A. L. Fitch, and Y. Liang, "A floating memristor emulator based relaxation oscillator," *IEEE Trans. Circuits Syst. I, Reg. Papers*, vol. 61, no. 10, pp. 2888–2896, Oct. 2014.
[40] Q. Yu, B. Bao, Q. Xu, M. Chen, and W. Hu, "Inductorless chaotic circuit based on active generalized memristors," *Acta Phys. Sin.*, vol. 64, no. 17, pp. 1–9, 2015.
[41] X. Zhong, M. Peng, C. T. Tse, S. Guo, and M. Shahidehpour, "Analysis and control of multiple chaotic attractors from a three-dimensional system," *Appl. Math. Comput.*, vol. 268, pp. 138–150, Oct. 2015.
[42] M. A. Zidan, H. Omran, C. Smith, A. Syed, A. G. Radwan, and K. N. Salama, "A family of memristor-based reactance-less oscillators," *Int. J. Circuit Theory Appl.*, vol. 42, no. 11, pp. 1103–1122, 2014.
[43] Q. Xu, Q. Zhang, B. Bao, and Y. Hu, "Non-autonomous second-order memristive chaotic circuit," *IEEE Access*, vol. 5, pp. 21039–21045, 2017.
[44] D. Yu, C. Zheng, H. H. C. Iu, T. Fernando, and L. O. Chua, "A new circuit for emulating memristors using inductive coupling," *IEEE Access*, vol. 5, pp. 1284–1295, 2017.

XIAOYUN ZHONG was born Shaoyang, Hunan, China, in 1991. She received the B.S. degree from the College of Mathematics and Econometrics, Hunan University, Changsha, China, in 2012, where she is currently pursuing the Ph.D. degree with the College of Electrical and Information Engineering. Her research interest includes power system stability and control, microgrids, and numerical analysis.

MINFANG PENG received the M.S. degree in electrical theory and the Ph.D. degree in electrical engineering from Hunan University, China, in 1991 and 2006, respectively. She is currently a Professor with the College of Electrical and Information Engineering, Hunan University. Her research interest includes smart distribution grid, intelligent information processing, electrical equipment monitoring and diagnosis, and electrical network analysis and diagnosis.

MOHAMMAD SHAHIDEHPOUR (F'01) received the Ph.D. degree in electrical engineering from the University of Missouri in 1983. He is currently the Bodine Chair Professor and the Director of the Robert W. Galvin Center for Electricity Innovation, Illinois Institute of Technology, Chicago, IL, USA. He is an academician of the U.S. National Academy of Engineering.

SHANGJIANG GUO received the Ph.D. degree in applied mathematics from Hunan University in 2004. He is currently a Professor and an Associate Dean with the College of Mathematics and Econometrics, Hunan University. His research interests center on bifurcation theory and its applications to differential equations. He was included as the "Most Cited Chinese Researchers" in mathematics by Elsevier from 2014 to 2017.